ELASTIC ANALYSIS OF CYLINDRICAL PRESSURE VESSELS WITH VARIOUS END CLOSURES

C. K. Ramesh, Tarun Kant & V. B. Jadhav

Indian Institute of Technology, Bombay, India

(Received: 15 February, 1974)

ABSTRACT

The well-known problem of the elastic analysis of cylindrical pressure vessels with hemispherical, torispherical and ellipsoidal heads, involving the partial differential equations for the classical theory of thin shells of revolution axisymmetric in character, is attempted here using a step-by-step integration procedure and a segmentation technique. The numerical results are obtained with a generalised computer program for a number of cases and for a given set of values of elastic moduli, Poisson's ratio and thickness/diameter ratio. The results are compared with the known results available in literature and also with the stresses predicted by the ASME Code.

NOTATION

E	Young's modulus
h	thickness of a shell
I	unit matrix
M_φ, M_θ	resultant bending moments per unit length of a shell
$M_{\varphi\theta}$, $M_{\theta\varphi}$	resultant twisting moments per unit length of a shell
K	extensional rigidity $= Eh/(1 - \gamma^2)$
D	flexural rigidity $= Eh^3/12(1 - \gamma^2)$
U	$1/R_\varphi + \gamma \sin \varphi/r$
N	number of segments in the integration path
n	number of variables in the system of differential equations
N_φ, N_θ	axial stress resultants per unit length of a shell
$N_{\varphi\theta}$, $N_{\theta\varphi}$	shearing stress resultants per unit length of a shell
p_φ, p_θ, p	components of surface loads
Q_φ, Q_θ	transverse shear resultants per unit length of a shell

Int. J. Pres. Ves. & Piping (2) (1974)—

r	distance of a point on the middle surface from the axis of revolution
R_φ, R_θ	principal radii of curvature of middle surface
s	distance measured from an arbitrary origin along the meridional direction
u, v, w	displacements of a shell middle surface in the φ, θ and normal directions
β	critical length factor
β_φ, β_θ	angle of rotation of normal
γ	Poisson's ratio
φ, θ	co-ordinates of a point of a shell
(A_j)	$[(n/2) \times 1]$ matrix of starting values of unknown variables
(T_{ij})	$[(n/2) \times (n/2)]$ coefficient matrix of known variables
(X_{ij})	$[(n/2) \times (n/2)]$ coefficient matrix of unknown variables

PROBLEM FORMULATION

The traditional method for the analysis and design of cylindrical pressure vessels having different types of end closures is essentially carried out using the well-known ASME Code[1] which is based on the classical membrane theory and involves many inconsistencies and consequent inaccuracies in the stresses and displacements, especially at the junctions. In the present study a numerical integration procedure, following Goldberg's[2] earlier work involving a segmentation technique, is attempted; to each of these segments a Runge–Kutta–Gill algorithm is applied to prevent any loss of accuracy arising out of the length of the curve over which the integration is carried out. A cylindrical pressure vessel having a hemispherical (Fig. 1), tori-spherical (Fig. 2) or ellipsoidal (Fig. 3) head has been considered for assessing the

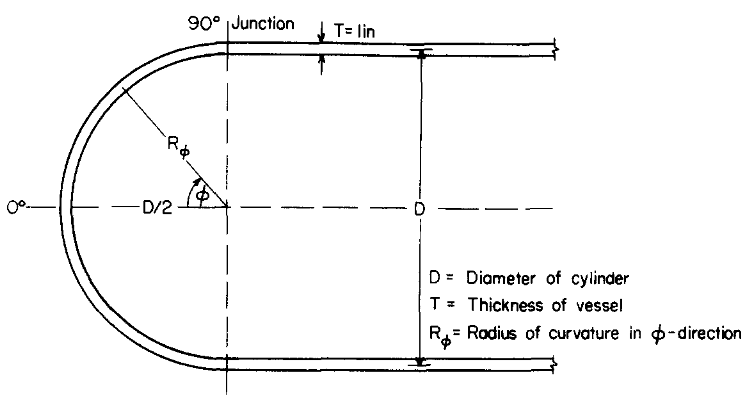

Fig. 1. Cylindrical vessel with hemispherical head.

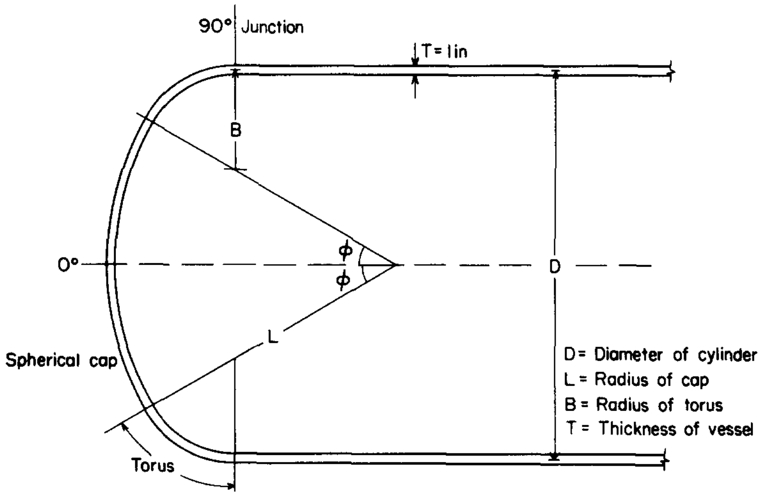

Fig. 2. Cylindrical vessel with torispherical head.

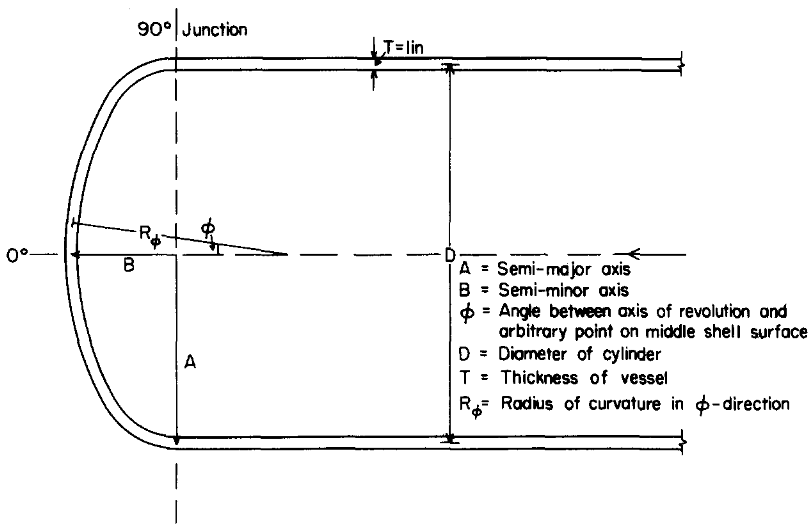

Fig. 3. Cylindrical vessel with ellipsoidal head.

applicability of this segmentation procedure in the context of some known results available from the literature[9,10] and also from the relevant clauses of the ASME Code. It is presumed that these results may form a reliable basis for the design of a cylindrical pressure vessel having the type of end closure considered here. The general program developed[6] in FORTRAN IV for the CDC 3600–160A computer system should also prove useful for any iterative type of design that may be required for practical considerations.

The fundamental equilibrium, strain–displacement and stress–strain equations describing the behaviour of a general shell, as derived by Reissner,[3] have been taken as the starting-point for the derivation of the following system of six first-

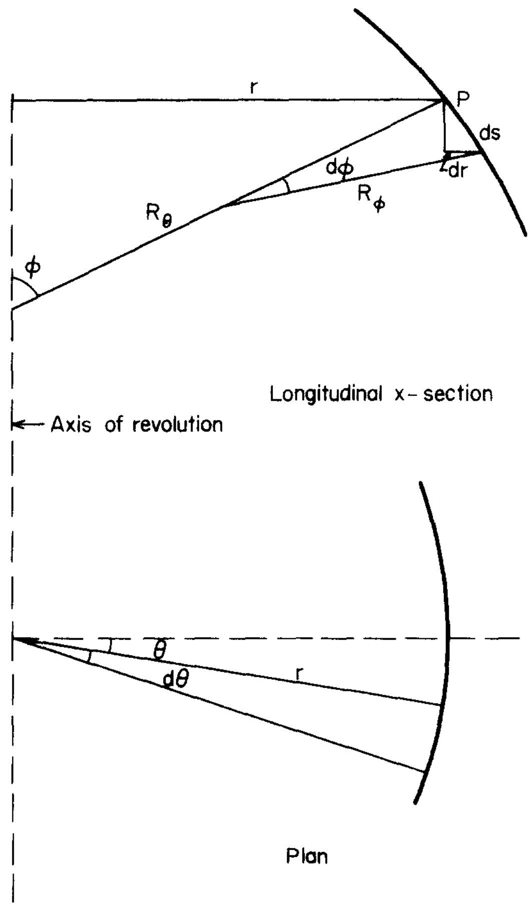

Fig. 4. Geometry of general shell surface.

order ordinary differential equations (eqns. (1) to (6)) governing the deformation of the shell of revolution (Figs. 4 and 5) with axisymmetric loading in terms of the six intrinsic variables which occur at the natural boundaries in the meridional direction (notations are given at the front of the paper):

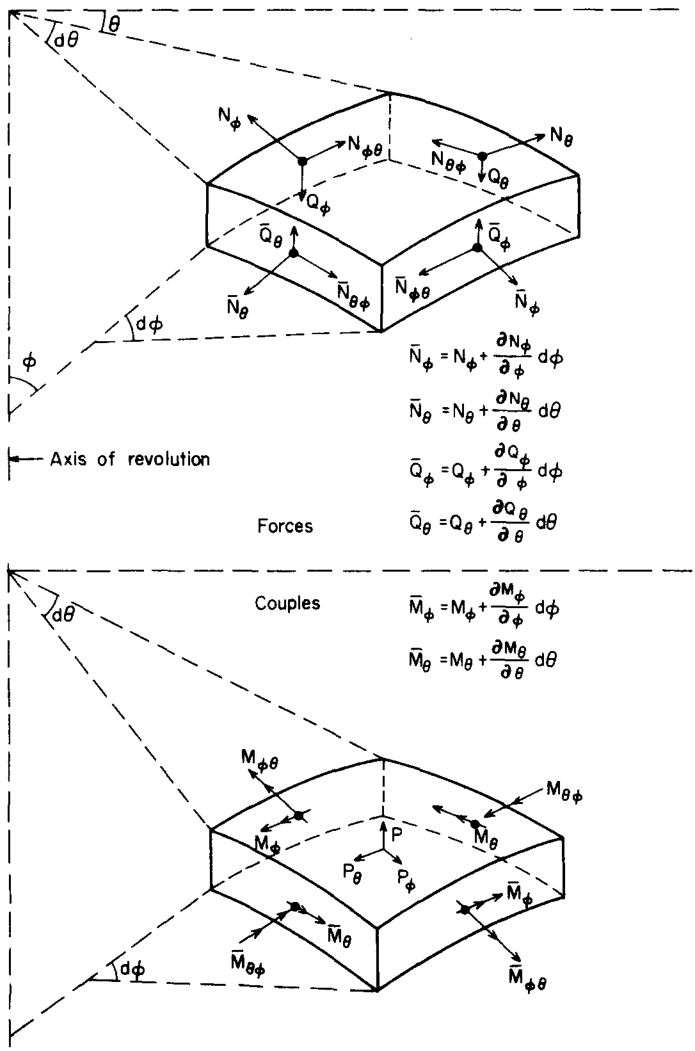

Fig. 5. Shell element.

$$\frac{\mathrm{d}w}{\mathrm{d}s} = \frac{1}{R_\varphi} u - \beta_\varphi \tag{1}$$

$$\frac{\mathrm{d}u}{\mathrm{d}s} = -Uw - \gamma \frac{\cos\varphi}{r} u + \frac{1}{K} N_\varphi \tag{2}$$

$$\frac{\mathrm{d}\beta_\varphi}{\mathrm{d}s} = -\gamma \frac{\cos\varphi}{r} \beta_\varphi + \frac{1}{D} M_\varphi \tag{3}$$

$$\frac{\mathrm{d}Q_\varphi}{\mathrm{d}s} = K(1-\gamma^2)\frac{\sin\varphi\cos\varphi}{r^2} u + K(1-\gamma^2)\frac{\sin^2\varphi}{r^2} w + UN_\varphi - \frac{\cos\varphi}{r} Q_\varphi - p \tag{4}$$

$$\frac{\mathrm{d}N_\varphi}{\mathrm{d}s} = K(1-\gamma^2)\frac{\cos^2\varphi}{r^2} u + K(1-\gamma^2)\frac{\sin\varphi\cos\varphi}{r^2} w - (1-\gamma)\frac{\cos\varphi}{r} N_\varphi - \frac{1}{R_\varphi} Q_\varphi - p_\varphi \tag{5}$$

$$\frac{\mathrm{d}M_\varphi}{\mathrm{d}s} = D(1-\gamma^2)\frac{\cos^2\varphi}{r^2}\beta_\varphi - (1-\gamma)\frac{\cos\varphi}{r} M_\varphi + Q_\varphi \tag{6}$$

along with the auxiliary relations:

$$N_\theta = \gamma N_\varphi + K(1-\gamma^2)\frac{(w\sin\varphi + u\cos\varphi)}{r} \tag{7}$$

$$M_\theta = \gamma M_\varphi + D(1-\gamma^2)\frac{\cos\varphi}{r}\beta_\varphi \tag{8}$$

Since the point on the axis of revolution is singular for a closed shell, special provision is made to specify the actual boundary condition at the axis of revolution in the meridional direction. For axisymmetric loads, the following three boundary conditions are applied at the apex of a fictitious aperture at the axis of revolution at both edges:

$$u = \beta_\varphi = Q_\varphi = 0 \tag{9}$$

SOLUTION AND RESULTS

The numerical integration technique as adopted here for the solution of the first-order ordinary differential equations (eqns. (1)–(6)), with the boundary conditions defined by eqn. (9), has the following distinct advantages over the other well-known methods: any general boundary conditions can be tackled and, depending

TABLE 1
PARAMETERS OF VARIOUS HEADS

Type of head	*Data used*	*Remarks*
1. Hemispherical	(a) $E = 3 \times 10^7$, $\gamma = 0{\cdot}3$ $D/T = 40{\cdot}0$, $0{\cdot}1°$ aperture at apex	Results reported in Table 2
	(b) $E = 3 \times 10^7$, $\gamma = 0{\cdot}3$ $D/T = 40{\cdot}0$, $1°$ aperture at apex	
	(c) $E = 3 \times 10^7$, $\gamma = 0{\cdot}3$ $D/T = 100{\cdot}0$, $0{\cdot}1°$ aperture at apex	
2. Torispherical	(a) $E = 65{,}000$, $\gamma = 0{\cdot}485$ $D/T = 44{\cdot}5$, $B/T = 13{\cdot}02$ $L/T = 31{\cdot}5$, $\varphi = 30°$ $0{\cdot}1°$ aperture at apex	Results reported in Table 3
	(b) $E = 3 \times 10^7$, $\gamma = 0{\cdot}3$ $D/T = 100{\cdot}0$, $B/T = 25{\cdot}00$ $L/T = 75{\cdot}00$, $\varphi = 30°$ $0{\cdot}1°$ aperture at apex	
	(c) $E = 3 \times 10^7$, $\gamma = 0{\cdot}3$, $D/T = 200$ $B/T = 25{\cdot}00$, $L/T = 175$, $\varphi = 30°$ $0{\cdot}1°$ aperture at apex	
3. Ellipsoidal	(a) $D/T = 40{\cdot}0$ Major axis/Minor axis $= 2{\cdot}0$ $0{\cdot}1°$ aperture at apex	Results reported in Table 4
	(b) $D/T = 80{\cdot}0$ Major axis/Minor axis $= 2{\cdot}0$ $0{\cdot}1°$ aperture at apex	
	(c) $D/T = 100{\cdot}0$ Major axis/Minor axis $= 2{\cdot}0$ $0{\cdot}1°$ aperture at apex	

upon the accuracy required, the step size in the integration process can be altered. Furthermore, the geometrical and material properties may be varied arbitrarily along the path of integration with any type of distributed or concentrated loading. For brevity, all the details of the segmentation technique and the use of the Runge–Kutta–Gill algorithm to each segment will not be highlighted here. A general program called PRESANLY involving maximum matrix size of 3×3 without any need for a large core memory size as required for other methods is made available; no trial runs are required as long as the length of each segment is less than the critical length of the shell. The input data to the program consist of number of variables and segments, segment length of each segment, number of increments in each segment, and angles which each segment makes with the axis of revolution, material and geometric properties. Maximum compilation and execution times for the various cases mentioned in Table 1 are 58 and 33 s respectively on the CDC 3600 computer.

DISCUSSION AND CONCLUSIONS

The discrete values of the meridional and circumferential stresses at the outer and and the inner fibres, the normal displacement and the shear in the shell for various degrees of location in the end closure and also at various points in the cylinder portion are presented for hemispherical, torispherical and ellipsoidal heads in Tables 2, 3 and 4 respectively. The results obtained are compared with known numerical results available in literature obtained by various other numerical methods for hemispherical and torispherical heads and are tabulated in Tables 5 and 6. Comparison with the ASME Code has been summarised in Table 7. The

TABLE 2
STRESS DISTRIBUTION IN CYLINDRICAL PRESSURE VESSEL WITH HEMISPHERICAL HEAD*
($0{\cdot}1°$ aperture at apex and $D/T = 40$)

Location	W ($\times 10^{-6}$ *in*)	Q ($\times 10^{-3}$ *lb*)	*Meridional stress* (*lb/in*^{2}) Outer	Inner	*Circumferential stress* (*lb/in*^{2}) Outer	Inner
1°	9·6960	0·75203	9·987	10·025	10·233	10·271
Apex	9·708	—	9·9948	10·001	9·9948	10·001†
30°	9·0474	1·9656	10·008	9·993	10·034	10·038
60°	7·0180	−25·994	9·9224	10·0474	9·7624	9·7624
90°	8·0018	434·30	10·008	9·994	15·005	15·001
Junction	7·999	—	10·007	9·9933	14·996	14·992†
3 in	10·419	−20·133	12·911	7·091	19·498	17·752
20 in	11·324	1·8975	9·987	10·015	19·986	19·986
40 in	11·333	−0·11488	9·999	10·003	20·000	20·000
End	11·33	—	9·9999	10·00	20·00	20·00†
Peak stress in cylinder			—	—	20·616	—
Peak stress in cylinder			—	—	20·627	—†

* *See* Fig. 1.
† Results obtained by Kalnin's method given in reference 4, p. 442.

TABLE 3
STRESS DISTRIBUTION IN CYLINDRICAL PRESSURE VESSEL WITH TORISPHERICAL HEAD*
($0{\cdot}1°$ aperture at apex, $D/T = 44{\cdot}5$, $B/T = 13{\cdot}02$, $L/T = 31{\cdot}5$, $\varphi = 30°$)

Location	W ($\times 10^{-2}$ *in*)	Q ($\times 10^{-2}$ *lb*)	*Meridional stress* (*lb/in*^{2}) Outer	Inner	*Circumferential stress* (*lb/in*^{2}) Outer	Inner
1°	9·9266	1·4721	16·398	16·764	17·029	17·397
Apex	—	—	16·976	13·9285	16·976	13·9285†
30°	3·3811	−76·162	13·326	15·528	7·81	5·39
60°	−0·90108	0·090625	5·615	18·059	−1·594	4·520
90°	2·4233	82·565	11·498	10·640	12·656	12·288
Junction	—	—	10·435	11·9705	12·393	13·060†
3 in	4·7068	−0·92313	17·485	6·753	22·230	16·056
20 in	5·7614	0·062357	11·029	11·209	22·178	22·266
40 in	5·7703	−0·016829	11·116	11·122	22·50	22·250
—	—	—	10·6355	10·0125	20·4255	21·760†
Maximum stress in head			22·235	—	—	—†
Maximum stress in head			19·580	—	—	—
Maximum stress in cylinder			—	—	24·24	—
Maximum stress in cylinder			—	—	23·585	—†

* *See* Fig. 2.
† Results obtained from reference 10.

torispherical head which had been analysed fulfils the 6% requirement of the Code. For hemispherical heads, both maximum meridional and circumferential stresses are within the limits of the Code requirements, but for torispherical heads, in two cases, the meridional (tensile) stresses exceed by an average of 33% the stresses predicted by the Code. The presence of high compressive stresses in the circumferential direction which may lead to buckling are not specified in the Code. Again, in the case of ellipsoidal heads, the stresses predicted by the Code are conservative

TABLE 4

STRESS DISTRIBUTION IN CYLINDRICAL PRESSURE VESSEL WITH ELLIPSOIDAL HEAD*

(0·1° aperture at apex, Maj/Min = 2·0, D/T = 40)

Location	*W* $\times 10^{-5}$ *in*	*Q* $\times 10^{-2}$ *lb*	*Meridional stress* (*lb/in*²)		*Circumferential stress* (*lb/in*²)	
			Outer	*Inner*	*Outer*	*Inner*
1°	4·4574	−1·2245	25·447	12·839	26·343	14·233
Apex	—	—	24·40	15·20	25·60	14·60†
30°	1·2813	−39·086	13·190	15·716	3·9770	−0·4612
60°	−0·51306	−28·132	−6·073	27·959	−10·952	−0·5416
90°	−0·071397	186·48	4·890	16·140	0·0961	3·7713
Junction	—	—	4·80	15·60	—	4·20†
3 in	0·73004	11·263	18·848	1·182	16·644	11·346
20 in	1·1301	0·71902	9·945	10·085	19·935	19·985
40 in	1·1330	−0·00015253	10·014	10·015	20·000	20·000
—	—	—	10·00	10·00	20·00	20·00†

* *See* Fig. 3.
† Results obtained from graphs given in reference 9.

TABLE 5

COMPARISON OF STRESSES IN CYLINDRICAL PRESSURE VESSEL WITH HEMISPHERICAL HEAD

(D/T = 40, length of cylinder = 40 in, internal pressure = 1 lb/in²)

	Finite difference CEGB program*	*Finite* element Bettis program*	*Numerical* integration Yale program*	*Authors' program*
Outside stress at apex (lb/in²)	9·9947	9·27	9·9949	9·987
Inside stress at apex (lb/in²)	10·002	9·77	10·001	10·025
Normal displacement ($\times 10^{-6}$ in)	—	9·3076	9·708	9·6960
Outside meridional stress at junction (lb/in²)	10·014	9·35	10·007	10·008
Inside meridional stress at junction (lb/in²)	9·9862	9·68	9·9933	9·9940
Outside circumferential stress at junction (lb/in²)	14·998	14·10	14·996	15·005
Inside circumferential stress at junction (lb/in²)	14·990	14·88	14·992	15·001
Normal displacement at junction ($\times 10^{-6}$ in)	7·996	7·857	7·999	8·0018
Rotation at junction ($\times 10^{-7}$ rad)	9·626	9·30	9·599	9·5827
Outside meridional stress at end (lb/in²)	10·00	9·27	9·9999	9·999
Inside meridional stress at end (lb/in²)	10·00	9·75	10·00	10·003
Outside circumferential stress at end (lb/in²)	19·999	19·07	20·00	20·00
Inside circumferential stress at end (lb/in²)	19·999	20·22	20·00	20·00
Normal displacement at end ($\times 10^{-6}$ in)	11·33	11·28	11·33	11·333
Peak stress (circumferential outside) (lb/in²)	20·624	20·24	20·629	20·63
Location, in from junction	6·5	9·2	6·44	

* Results taken from reference 8, p. 23, and also from reference 4, p. 442.

and the deviation in the calculated stresses is about 30%. The high compressive stresses in the region of 65° are not recognised by the Code. The Code does not state whether the stress is meridional or circumferential, or whether it is tensile or compressive. In most cases the Code attempts to predict only the direct (membrane) stresses due to internal pressure. The stress magnification factor (K) in the ASME Code formula apparently underestimates the stresses in the case of torispherical and ellipsoidal heads.

The comparison of the three heads for $D/T = 100$ (Figs. 6 and 7) indicates that the circumferential (outer) compressive stresses in the ellipsoidal head are two and a half times greater than the torispherical heads. The meridional (outer) stresses in the torispherical head are tensile, whereas a small portion of the ellipsoidal

TABLE 6
STRESS INDEX FOR TORISPHERICAL HEAD
(Stress index I = Stress/($PD/2T$), D/T = 44·50)

Stress index	*Test results*	*Bettis program (finite element)*	*% error*	*CEGB program (finite diff.)*	*% error*	*Authors' results*	*% error*
$I_\varphi = I_\theta$ outer at apex	0·763	0·708	−7·1	0·734	−3·8	0·752	−1·44
$I_\varphi = I_\theta$ inner at apex	0·626	0·732	17·0	0·752	20·0	0·767	22·55
I_φ inner at junction	0·538	0·314	−41·7	0·485	−9·8	0·478	−11·1
I_φ outer at junction	0·469	0·634	35·0	0·515	10·0	0·516	10·2
I_θ inner at junction	0·587	0·566	−3·5	0·552	−5·8	0·552	−5·8
I_θ outer at junction	0·557	0·698	25·2	0·567	1·6	0·568	1·7
I_φ inner at end	0·450	0·489	8·7	0·500	11·0	0·498	10·6
I_φ outer at end	0·478	0·467	−2·5	0·500	4·2	0·499	4·1
I_θ inner at end	0·978	1·01	3·2	1·00	2·2	1·00	2·2
I_θ outer at end	0·918	0·956	4·0	1·00	8·8	1·00	8·8
I_{max} in head	0·880	0·908	3·1	0·904	2·7	0·980	12·5
I_{max} in cylinder	1·06	1·04	−1·8	1·089	2·8	1·08	2·6

TABLE 7
COMPARISON WITH ASME CODE

Type of head	*D/T*	*Stress predicted by ASME Code (lb/in²)*	*Maximum stress in the present study*	
			Meridional (lb/in²)	*Circumferential (lb/in²)*
Hemispherical	40·0	21·15	12·649 (inner) at 85°	15·005 (outer) at junction
	100·0	50·65	32·321 (inner) at 85°	37·509 (outer) at junction
Torispherical	44·5	17·75	22·235 (outer) at 20°	−1·755(outer)atjunction
	100·0	39·0	55·063 (outer) at 25°	−13·705 (outer) at 50°
	200·0	221·0	212·253 (inner) at 40°	−197·39 (outer) at 50°
Ellipsoidal	40·0	20·1	+28·168 (inner) at 65°	−10·95 (outer) at 65°
	80·0	40·1	53·249 (inner) at 70°	−29·318 (outer) at 65°
	100·0	50·1	65·217 (inner) at 70°	−39·332 (outer) at 65°

+ Tensile stress.
− Compressive stress.

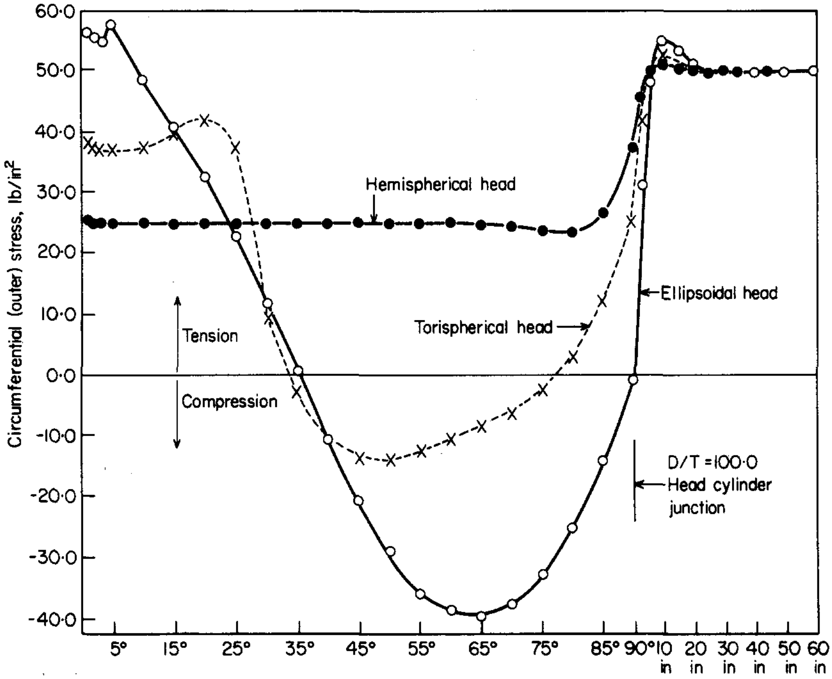

Fig. 6. Circumferential stress distribution.

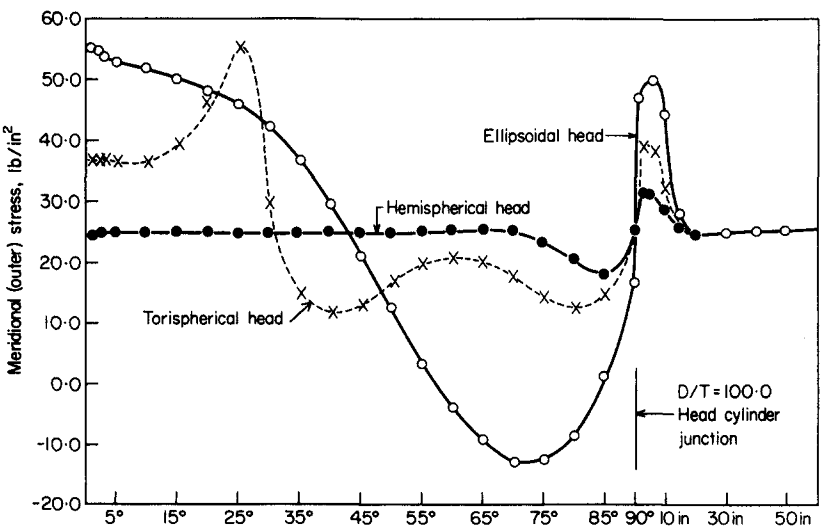

Fig. 7. Meridional stress distribution.

head is under compressive stresses. It is also seen that in the case of torispherical heads, high compressive stresses are induced in the circumferential direction in the region of 45° to 50°, whereas in ellipsoidal heads it is in the region of 60° to 65°. In both cases the head deflects inward from 45° to 90°.

REFERENCES

1. Rules for Construction of Pressure Vessels, Division 1 and Division 2: Alternative Rules, ASME Boiler and Pressure Vessel Code, Section VIII, American Society of Mechanical Engineers, New York, 1971 ed.
2. Goldberg, J. E., Setlur, A. V. & Alspaugh, D. W. Computer analysis of non-circular cylindrical shells, Conference of the International Association for Shell Structures (IASS), Budapest, 1965.
3. Reissner, E. A new derivation of the equations for the deformations of elastic shells, *American Journal of Mathematics*, **63** (1941) p. 177.
4. Kraus, H. *Thin elastic shells*, Wiley, New York, 1967.
5. Ralston, A. & Wilf, H. S. *Mathematical methods for digital computers*, Wiley, New York, 1960.
6. Jadhav, V. B. Elastic analysis of cylindrical pressure vessels with various end closures, M. Tech. Dissertation, Department of Civil Engineering, Indian Institute of Technology, Bombay, 1972.
7. Gill, S. S. *The stress analysis of pressure vessels and pressure vessel components*, Pergamon Press, Oxford, 1970.
8. Kraus, H. A review and evaluation of computer programs for the analysis of stresses in pressure vessels, Welding Research Council Bulletin No. 108, 1965, p. 11.
9. Kraus, H. Elastic stresses in pressure vessel heads, Welding Research Council Bulletin No. 129, 1968, p. 1.
10. Kraus, H. A comparison of measured and calculated stresses in pressure vessels, *Trans. ASME*, **89A** (1967) p. 341.